JOURNAL OF PROPULSION AND POWER
Vol. 12, No. 4, July–August 1996

Shock Initiation of Crystalline Boron in Oxygen and Fluorine Compounds

Herman Krier,* R. L. Burton,† S. R. Pirman,‡ and M. J. Spalding‡
University of Illinois at Urbana–Champaign, Urbana, Illinois 61801

The ignition delay and combustion of amorphous and crystalline boron particles is investigated at elevated temperatures and pressures for wet, dry, and fluorine-containing atmospheres. Micron-sized amorphous and sieved 20-μm crystalline particles are ignited in the reflected-shock ambient conditions produced at a shock-tube endwall. The ignition delay and combustion times are examined as a function of temperature for pressures of 8.5, 17, and 34 atm and for oxidizer mixtures of 100% oxygen, 30% water vapor, 1–3% sulfur hexafluoride, and 6–12% hydrogen fluoride. At 8.5 atm, SF_6 has little effect on the ignition delay or temperature limit for 20-μm particles, but at 34 atm the effect of SF_6 is to reduce both the ignition delay time and the ignition temperature limit, from 1900 to 1400 K. In addition, experiments conducted with 1- and 20-μm crystalline boron particles and with unsieved <200-μm B_2O_3 particles show that the first and second peaks observed in 20-μm particle combustion are associated with removal of the oxide layer.

Introduction

THE potential of high-energy density materials to achieve a controlled high-energy release has instigated extensive research on liquid and solid propellant combustion applications. Whether the energetic material is used for rocket propulsion or detonation purposes, performance increases are always a major goal. A concentrated effort has also been placed on studying metallized solid propellant combustion, which can yield large amounts of energy per unit volume. Currently, aluminum and magnesium are the metals of choice, although boron produces an even higher energy release. In this article research is presented on boron combustion with various oxidizers at high pressures.[1]

Benefits of Boron as a Fuel

Boron has great potential for use as an additive energetic material. Apart from being a relatively common element, it has the greatest heating value of any fuel except beryllium, which reacts with oxygen to form extremely toxic BeO. Boron can also be used for controlled, nonideal detonations. Its high-energy output coupled with a delayed reaction generates an increased pressure–volume process, which results in more work output.

Disadvantages of Boron as a Fuel

For a material to be a viable candidate for a fuel or fuel additive, it must be able to ignite, burn, and release its energy within the combustor region of a rocket motor. Unfortunately, the ignition delay and combustion times for boron may not meet this criterion for most applications.[2] The main reason that boron is difficult to ignite is that the particle is coated with an oxide layer of B_2O_3.

The B_2O_3 layer, present whenever the particle is in an oxygen-containing atmosphere, inhibits further oxidation of the particle and therefore restricts the ignition process. Above a particle temperature of 723 K, the oxide layer liquefies. This allows some oxygen to diffuse slowly through the liquid layer and react with the boron. However, the reaction then produces more oxide and increases the thickness of the oxide layer, which retards the diffusion process as well as the combustion of the particle.

In addition, full utilization of energy from the combustion reaction is difficult to achieve because a significant fraction of the energy is never released. Because boron has high melting and boiling temperatures, the heating of the particle can continue for a time longer than the residence time in a combustor. If the particle happens to react completely, most of the products formed will be in the gas phase. Highest energy output is not achieved until the products condense to liquid phase. Since the boron product condensation process is relatively slow until the temperature drops significantly, the benefits of product condensation are usually never realized.[2,4] The trapping of the products in the gas phase can potentially reduce the heating value of boron by up to 25%.

Comparison of Boron with Aluminum

Other solid fuels have qualities similar to boron, so that it would seem that the combustion process might also be similar. For instance, aluminum, which is in the same group on the periodic table as boron and has been utilized extensively for rocket propulsion, also forms an oxide layer upon heating, which is similar to the structure of boron oxide (Al_2O_3 and B_2O_3). Table 1 lists some of the properties of boron and aluminum and their oxides. However, the two elements and their oxides display significantly different melting and boiling temperatures and enthalpy of fusion (Table 1). There is consequently little in common in their ignition processes.[2,5]

The ignition and combustion of aluminum has been studied extensively by many researchers, including Roberts et al.,[5,6] who conducted their shock-tube experiments with a similar configuration used for the present boron research. For aluminum, an oxide layer forms during heating in an oxygen-containing atmosphere. Before the aluminum melting point is reached, the aluminum expands and the oxide layer breaks apart allowing oxygen to reach the aluminum particle.[5] As the particle temperature increases to the melting point of the oxide, the oxide layer retracts to expose the bare particle and allows

Presented as Paper 95-2120 at the AIAA 29th Thermophysics Conference, San Diego, CA, June 19–22, 1995; received June 29, 1995; revision received Jan. 22, 1996; accepted for publication Feb. 2, 1996.

*Professor, Department of Mechanical and Industrial Engineering. Fellow AIAA..
†Associate Professor, Department of Aeronautical and Astronautical Engineering. Associate Fellow AIAA.
‡Research Assistant, Department of Mechanical and Industrial Engineering. Student Member AIAA.

Table 1 Physical properties of Am.[a] and Cr.[b] boron, aluminum, and their oxides, B_2O_3 and Al_2O_3

Physical property	B-Am.	B-Cr.	B_2O_3	Al	Al_2O_3
ρ, kg/m^3	2220 (Ref. 3)	2350 (Ref. 7)	2990 (Ref. 12)	2700 (Ref. 8)	3980 (Ref. 8)
κ, W/m K at 300 K	27.6 (Ref. 10)	27.4 (Ref. 7)	——	237 (Ref. 8)	36 (Ref. 8)
κ, W/m K at 800 K	8.1 (Ref. 10)	7.36 (Ref. 12)	——	218 (Ref. 8)	10.4 (Ref. 8)
c_p, J/kgK at 300 K	1116 (Ref. 12)	1055 (Ref. 9)	1026 (Ref. 7)	903 (Ref. 8)	765 (Ref. 8)
c_p, J/kgK at 800 K	——	2144 (Ref. 12)	1863 (Ref. 9)[c]	1146 (Ref. 8)	1180 (Ref. 8)
T_{mp}, K	——	2350 (Ref. 9)	723 (Refs. 7 and 9)	933 (Ref. 12)	2327 (Ref. 12)
T_{bp}, K	——	4138 (Ref. 9)	2316 (Refs. 9 and 11)	2791 (Ref. 12)	3253 (Ref. 12)
T_{ign}, K	1073 (Ref. 13)	1950 (Ref. 11)	——	2327 (Ref. 5)	——
H_{fus}, kJ/mol	——	50.2 ± 1.7 (Ref. 9)	24.1 ± 0.4 (Ref. 9)	10.7 ± 0.2 (Ref. 9)	111 ± 4 (Ref. 9)
H_{vap}, kJ/mol	——	480 (Ref. 9)	——	294 (Ref. 9)	——
MW, kg/kmol	10.81 (Ref. 12)	10.81 (Ref. 12)	53.62 (Ref. 12)	26.98 (Ref. 12)	101.96 (Ref. 12)

[a]Amorphous. [b]Crystalline. [c]At 723 K.

a vigorous ignition reaction between the liquid aluminum particle and the oxidizer. The liquid droplet has a detached gas phase envelope where homogeneous combustion of the particle occurs. To complete the process, the product Al_2O_3 condenses out, releasing the additional enthalpy of vaporization.

Boron particle ignition follows a completely different process. After initial particle heat-up, the oxide layer melts long before the boron particle melts (Table 1). This allows the oxidizer to diffuse through the oxide layer and react with the particle, starting the ignition process. The oxide layer then builds up, retarding further oxidation. As the particle temperature increases further, the oxide begins to evaporate, removing energy from the particle. At a certain point the energy released from the chemical reaction exceeds the energy absorbed from evaporation and heat loss, and the remaining oxide suddenly evaporates. The particle then reignites and heterogeneously combusts. It is difficult to achieve homogeneous gas phase combustion of the boron particle because the boron boiling point is relatively high (Table 1), so that the combustion reaction consists mainly of surface reactions. Because the product B_2O_3 remains in the gas phase, the benefits of energy release from condensation are lost in rocket motor applications.

Research Background

Because the benefits of boron-based combustion are apparent, research continues on how to exploit its advantages. There are numerous experiments reported that study the ignition process and attempt to establish a starting database for boron ignition and combustion models.

In 1982, King[2] reviewed several models and described the basic boron particle combustion process. Figure 1 shows a diagram of boron particle processes during heating.[14] It has been theorized[15] that the intermediate species BO and BO_2 are slow to react to form B_2O_3, resulting in the long ignition delays observed in the experiment. Others have hypothesized that those species are not intermediate, but are final products. Yeh and Kuo state that the rate-limiting step is the combination of gaseous O_2 with a $(BO)_n$ polymer to form gaseous BO_2 and adsorbed oxygen.[14] The general consensus is that faster removal of the oxide layer will decrease ignition delay times.

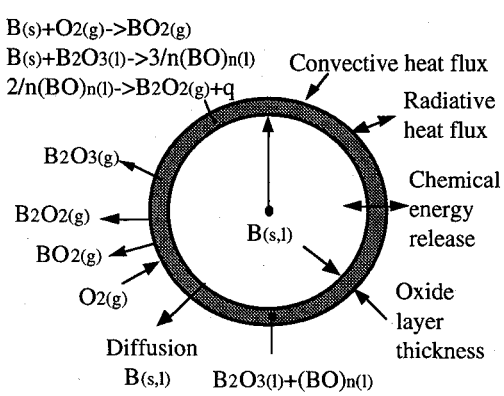

Fig. 1 Ignition model of boron particle showing various processes that occur during particle heating.

Experimental evidence has shown a reduction in ignition delay in atmospheres containing water vapor.[16,17] Other experiments have shown a reduction in ignition delay for atmospheres containing other compounds, such as species containing fluorine.[18] These chemical reactions release gaseous products such as HBO_2, or possibly OBF. However, these models are difficult to evaluate because there is little supporting experimental data.

The present study expands the boron ignition database to include the ignition of boron particles in oxygen at pressures ranging from 8.5 to 34 atm, and in gases containing SF_6/O_2 and HF/O_2 mixtures. The first compound is utilized to study the effect on boron ignition of fluorine atoms, which may increase the energy output of boron combustion as well as reduce its ignition delay. Sulfur hexafluoride dissociates easily at relatively low temperatures (<2000 K), providing an excellent source of fluorine atoms. Hydrogen fluoride does not dissociate easily, and so the complete molecule must interact with the boron particle. It has been proposed that the HF molecule will reduce the particle ignition delay even further.[19]

Experimental Technique

The experiments consisted of igniting and combusting 1–50-μm boron particles with various oxidizers at the endwall of a 12-m shock tube.[1,5,20] The endwall region is well suited for particle combustion studies, since the flow velocity is nearly zero. The main limitation of this technique is the short duration of the test conditions because of the arrival of pressure disturbances from the interaction of the reflected shock wave and the flow contact surface. In these experiments, the pressure disturbances do not arrive until after the ignition event has ended.

To create the desired conditions, the shock-tube driver section is filled with high-pressure gas (condition 4), and the 8.9-cm-diam driven section with a low-pressure gas (condition 1). All conditions are depicted in Fig. 2. Details of the gasdynamics equations utilized to solve for P_5 and T_5 for a given P_4/P_1 are presented elsewhere.[5,6]

Experimental Procedure

The 8.4-m-long driven section is coupled to a 3.3-m-long, 16.5-cm-diam stainless-steel driver section by a converging nozzle/dual-diaphragm section with Mylar diaphragms. A reduced diameter driven section provides an efficient steady expansion and also reduces the driver pressure necessary to produce given test conditions, compared to a constant area shock tube.[21]

The boron particles are held with a small amount of finger oil on a hobby knife blade mounted 8 mm from the endwall (Fig. 3). The endwall houses a quartz/polycarbonate composite window that allows emitted radiation to be monitored with a

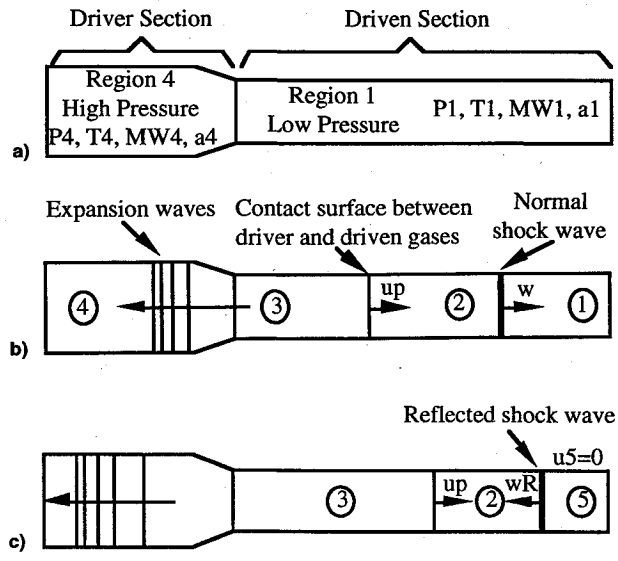

Fig. 2 Conditions in a shock tube a) initially, b) after diaphragm is broken, and c) after the shock wave reflects from the endwall.

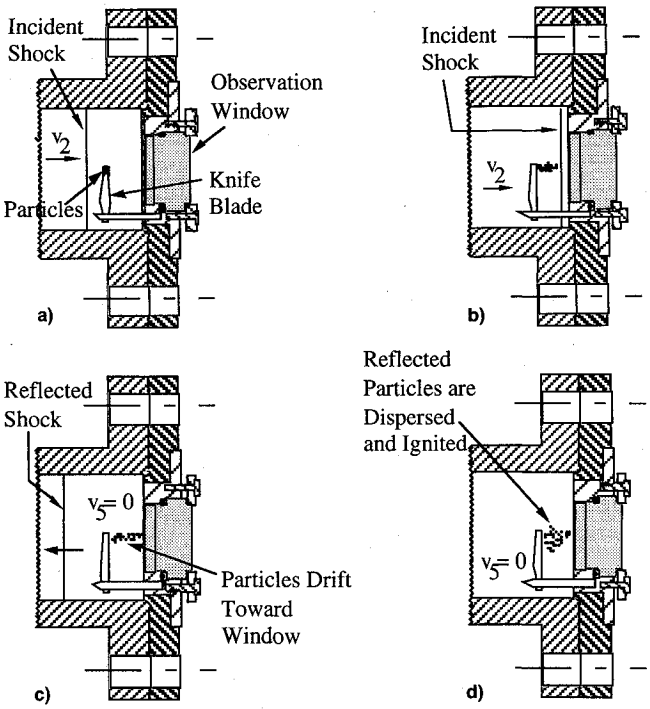

Fig. 3 Particle mounting technique and particle dispersal from incident and reflecting shock waves. Knife blade is located 8 mm from endwall. The window is quartz/polycarbonate composite, with the 6.35-mm-thick quartz window in contact with the reflected shock.

photodiode mounted outside of the shock tube. The particles are blown off the knife blade toward the endwall by the high-velocity flow behind the incident shock wave. After the reflected shock passes, the particles drift in the stagnant gas and collide with and reflect off the endwall. The particles are then ignited (Fig. 3) and are sufficiently dispersed so that the radiation from a hot particle does not contribute to the heating of adjacent particles, making the experimental results independent of the number of combusting particles.[5,6]

Various procedures are followed for filling the driven section, depending on the oxidizer.[1] Oxygen is admitted as a gas. Water vapor and SF_6 are admitted by evaporation of the liquid phase. Hydrogen fluoride (HF) requires special precautions. Because it is a corrosive gas, the HF bottle is stored in a fume hood. An NaOH scrubber is used to neutralize combustion products before being discharged to the atmosphere. A dry nitrogen flushing system drives the hydrogen fluoride out of the shock tube, which is made HF resistant with Teflon® seals. The HF etches the quartz window, which is replaced when corrosion becomes excessive.

For HF, the tube is first filled with nitrogen to approximately 650 kPa. This step allows for the detection of leaks and purges moisture from the system when the nitrogen is vented off. After filling to the desired partial pressure of oxygen, hydrogen fluoride is introduced into the tube with a fast-acting solenoid and an air-lock valve arrangement, which prevents large amounts of evaporating liquid HF from entering. After the hydrogen fluoride is injected, it reacts with the wall and plates out, reducing the pressure. The injection procedure is repeated until no pressure drop is observed in the driven section.

Experimental Data

The data required from the shock tube are the conditions of the gas behind the reflected shock and the time it takes the boron to ignite and burn. The temperature and pressure are calculated from the initial driver conditions and the velocity of the incident shock wave, measured with piezoelectric pressure transducers located on the sidewall and endwall of the shock tube, and recorded on a Soltec ADA-1000 8-bit, 10-MHz digital oscilloscope. The signals from the endwall and sidewall transducers are depicted in Figs. 4a–4c. A more detailed description of the procedure is given in Ref. 6.

The average of the velocity between the sidewall transducers and the velocity between the last sidewall transducer and the endwall is used as the shock-wave velocity. The incident Mach number is determined from the initial sound speed. The Mach number and initial pressure and temperature of the driven section allow the final pressure and temperature to be calculated.[5,6,22]

The ignition and burning of the particles is recorded with a Motorola MRD500 semiconductor photo detector, which is sensitive in the wavelength region 0.35–1.25 μm, with a peak sensitivity at 0.8 μm. The particle radiation is collected with an 80-mm-diam aspheric collecting lens, reflected off a first-surface mirror, and is focused onto the photodiode. A typical photodiode signal is shown in Fig. 4d, and displays a three-peak structure.

Boron Particles

Two types of boron particles are used. The primary supply is a crystalline boron purchased from Aldrich Chemical Company, Inc., with a size range of 45 μm or less and a quoted purity of 99%. For the tests to yield comparable results, the powder is sifted into specific size ranges with a Gilson vibrating shaker employing U.S. Standard sieves with mesh openings of 45, 38, 32, 25, and 20 μm, respectively. The stated tolerance of all mesh openings is ± 3 μm.

Photographs of the particles (Fig. 5) were taken with a scanning electron microscope (SEM), which confirm the presence of larger crystalline particles with smaller (<1-μm) parasitic particles stuck to the surface. The diameter of the larger particles is measured by the sedimentation technique with a Horiba CAPA-700 Particle Analyzer with glycerin as the dispersion fluid. Because the standard deviation is large and because measurements of many samples from the same size range resulted in a range of mean effective diameters, the particles are designated by the size of the sieve (e.g., 20 μm).

The second particle type is an amorphous boron purchased from the Johnson Matthey Catalog Company. Amorphous particles are actually agglomerates of smaller (<1-μm) particles. An SEM photomicrograph shows that these particles range in size up to 7 μm.

Operating Conditions

Operating limits are determined from the structural design of the shock tube, which is rated for 100 atm in the driver

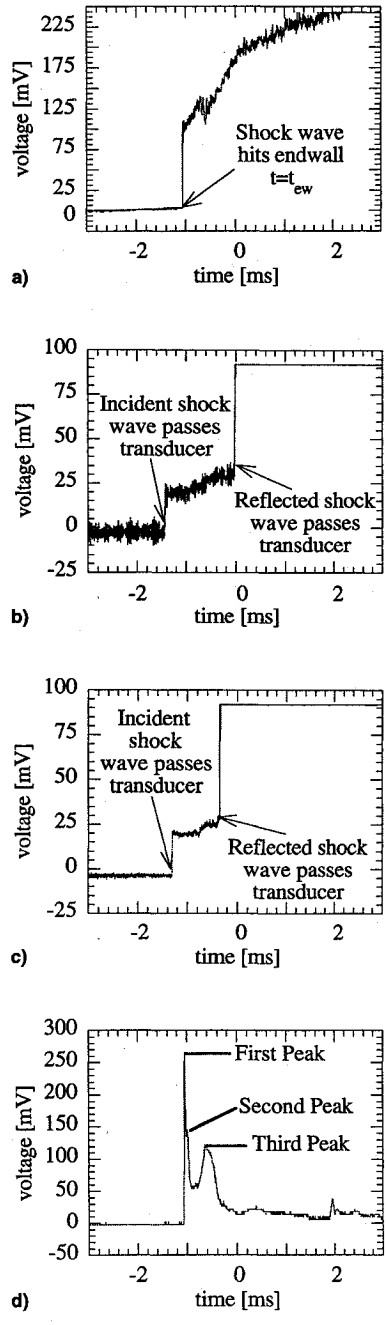

Fig. 4 Typical boron signals from a) endwall pressure transducer, b) first sidewall pressure transducer, c) second sidewall pressure transducer, and d) photodiode. The photodiode signal displays three peaks. All ignition times are referenced from t_{ew} in a).

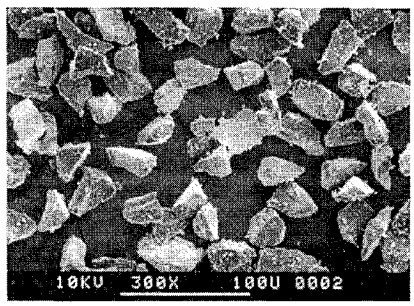

Fig. 5 Photomicrograph of 20–25-μm crystalline boron particles with attached submicron parasitic particles, at 300× magnification. White micron bar length is 100 μm.

section. If oxygen is used, this corresponds to a test pressure of 34 atm and a temperature around 3000 K (Ref. 6). Higher temperatures can be obtained if the desired test pressure is reduced below 34 atm. If other oxidizer gases are used, the test conditions change to account for the different molecular weights and different rates of dissociation. The initial ignition delay experiments with boron utilized 100% oxygen. The results from these tests were then used as the basis for comparison with experiments in which other gases were added to the oxygen.

The pure oxygen tests were used to indicate the boron particle size best suited for the experiments. Transient heating calculations were conducted to show that 45-μm boron particles would ignite within 1 ms in gas temperatures of 3000 K. The size range available (20–25 μm) was therefore judged appropriate for a majority of the experiments. The initial experiments confirmed that 20-μm particles ignited in less than 1 ms in a range of gas temperatures of 1900–3100 K.

Water vapor was the first oxidizer additive employed. Previous experiments[16] with boron and water vapor used water vapor mole fractions between 0.20–0.30, with the remaining gases consisting of a mixture of oxygen and carbon dioxide. The present research used 30% water vapor and 70% oxygen.

Sulfur hexafluoride was added to the oxygen in later experiments. A majority of these experiments were conducted with 1% SF_6 added to 99% oxygen. Hydrogen fluoride was also tested, keeping the number of hydrogen fluoride molecules the same as the number of fluorine atoms in the sulfur hexafluoride experiments. Calculations show that dissociation of HF at the temperatures studied is less than 1%. HF/O_2 fractions of 6/94 and 12/88% were tested.

Experimental Results

Ignition delay and combustion time results for the shock-tube experiments were determined as a function of temperature, pressure, and particle size for each oxidizer mixture. The empirical measurement of these times is illustrated in Fig. 6, in which t_{ign} is defined as the numerical average of the times of three waveform features: 1) base, 2) half, and 3) peak, where t_H is the time at which the voltage is halfway between base and peak voltage. The extinction time $t_{extinct}$ is found from the average of three times on the downward slope. The burning or combustion time is found by subtracting t_{ign} from $t_{extinct}$.

Amorphous Boron

An investigation of amorphous boron ignition delay vs temperature for different pressures and oxidizers was conducted. The temperature range was 1400–2800 K. A typical broadband photodiode signal for amorphous boron is shown in Fig. 7, with time referenced to the shock-arrival time at the endwall. All experiments with amorphous boron display a similar signal with a single voltage peak.

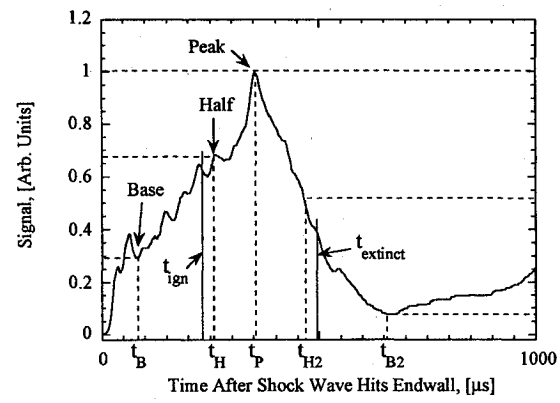

Fig. 6 Boron emission signal at 3100 K illustrating definitions for ignition and extinction time.

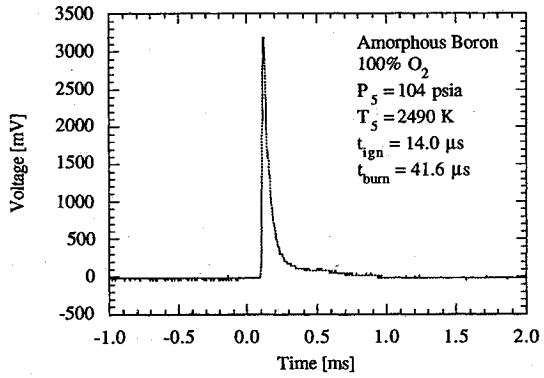

Fig. 7 Typical amorphous (~1 μm) boron emission signal in pure oxygen showing the characteristic single voltage peak.

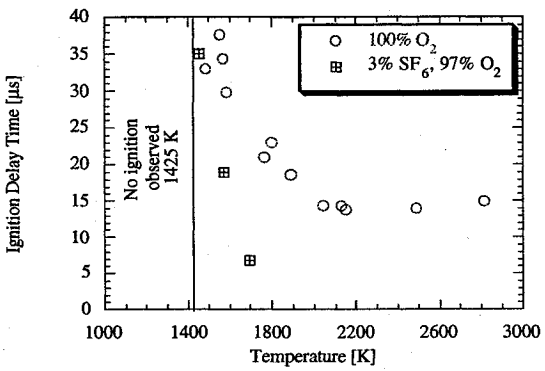

Fig. 8 Amorphous boron ignition delay vs temperature for two oxidizers at a nominal pressure of 8.5 atm.

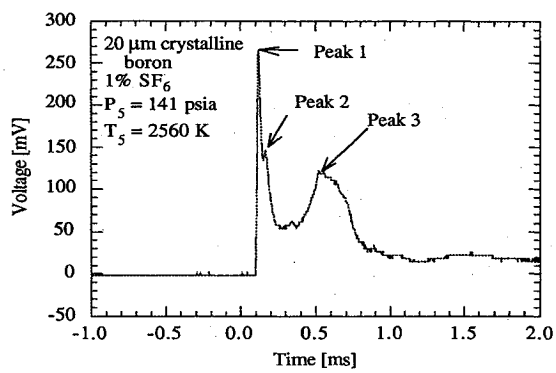

Fig. 9 Typical crystalline boron emission signal at 2560 K showing the characteristic three-peak signal.

The nominal condition to which all results are compared (Fig. 8) is a reflected pressure of 8.5 atm of a 100% oxygen atmosphere, showing an ignition limit of 1425 K. Use of 3% oxidizer SF_6 reduces ignition delay time slightly from that for pure O_2.

Crystalline Boron

As with the amorphous boron experiments, nominal conditions for crystalline boron are set at 8.5 atm with 100% oxygen, using 20-μm particles. The signal time history for 20-μm crystalline boron (Fig. 9) is more complex than for amorphous boron particles (Fig. 7). For the oxygen experiments, most signals show three peaks and ignition delays are measured for all three. The first peak appears in all tests above 1800 K. It was originally thought that the first peak was because of the presence of parasitic particles on the crystalline particles (Fig. 5), but this hypothesis was disproved by ignition tests at 3100 K and 8.5 atm using 1- and 20-μm crystalline boron particles, and unsieved (<200-μm) particles of B_2O_3. The first 100 μs of the emission data from the tests are shown in Fig. 10, normalized in amplitude to the second peak, and display similar time histories for all three types of particles.

The smaller 1-μm crystalline particles show the same behavior as the 20-μm particles for the first two peaks, which tends to support the parasitic particle hypothesis. However, the B_2O_3 particles also show the same behavior, and since B_2O_3 particles do not have parasitic boron particles attached, it now seems more likely that the first two peaks are the result of oxide evaporation.

The second peak is not present in all cases. It appears consistently in the pure oxygen experiments, always attached to the first peak as shown. It also is present in a majority of the water vapor/oxygen experiments. However, in almost all of the SF_6/O_2 tests, the second peak is nonexistent.

Figure 11 depicts the ignition delay vs temperature trend for the first and second peaks at 8.5 atm. The 34-atm data are similar and are not shown. The ignition temperature limit for the first two peaks is approximately 1900 K. There is a good deal of scatter in the first peak data and less for the second peak data. Data for both peaks show a trend of decreasing delay time with increasing temperature. This would indicate the oxide layer removal rate increases with temperature, as would be expected.

Third peak ignition delay times for 20-μm boron in 100% O_2 at 8.5 and 34 atm are shown in Fig. 12. The data display an ignition temperature limit of 1900 K, which is in agreement with other research.[23] There is a small pressure effect at temperatures below 2600 K and a decrease in ignition delay time with increasing temperature, with an average ignition delay time of about 250 μs at 3000 K.

The burning time for 20-μm boron particles is shown as a function of temperature in Fig. 13 at 8.5, 17, and 34 atm. The

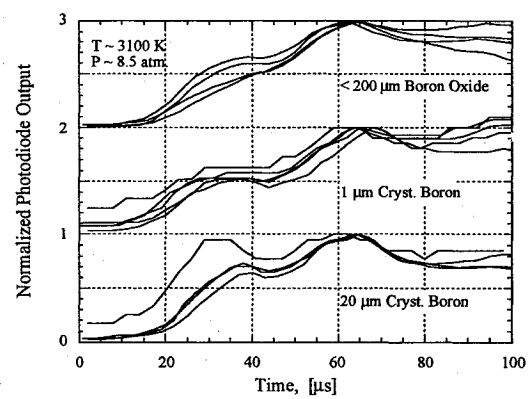

Fig. 10 First 100 μs of emission data from amorphous boron oxide and crystalline boron particles. Data are normalized to the second peak for each experiment shown.

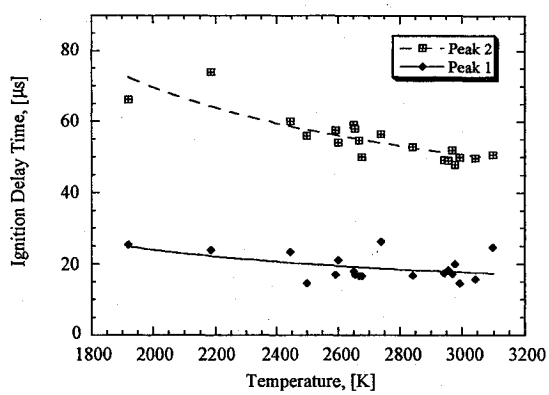

Fig. 11 Ignition delay time vs temperature of the first and second peaks in 100% oxygen atmosphere at 8.5 atm for a 20-μm crystalline boron particle sample.

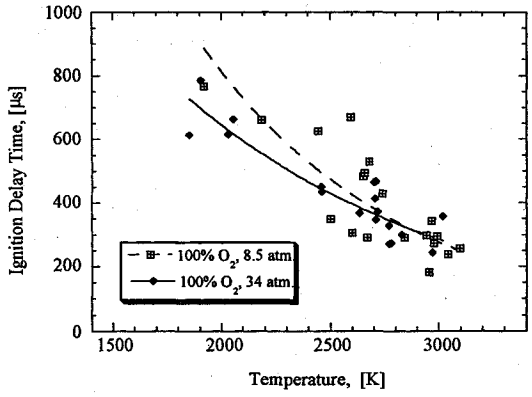

Fig. 12 Third peak ignition delay time vs temperature in 100% oxygen atmosphere at 8.5 and 34 atm for 20-μm crystalline boron particles.

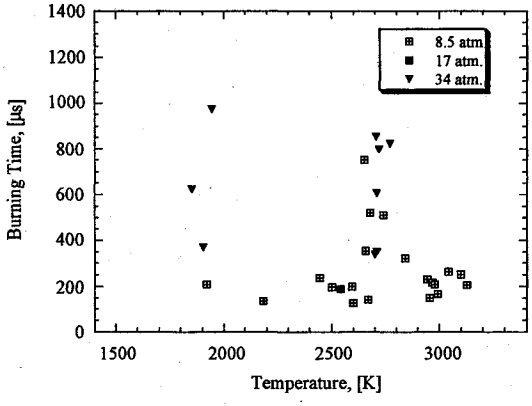

Fig. 13 Burning time vs temperature of the third peak in 100% oxygen atmosphere for 20-μm crystalline boron particles at pressures of 8.5, 17, and 34 atm.

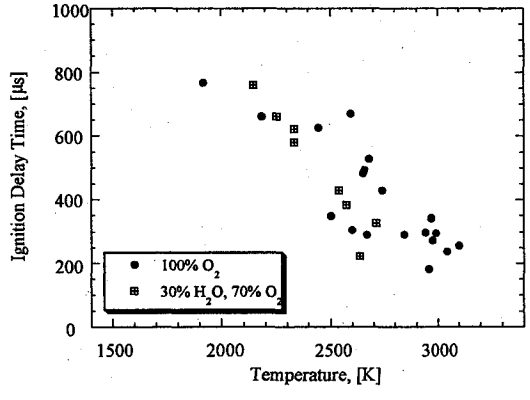

Fig. 14 Third peak ignition delay time vs temperature, comparing water vapor and oxygen for 20-μm boron particles at 8.5 atm.

shortest burning time measured is 200 μs, whereas the longest approaches 1.0 ms. There is a great deal of scatter in this data and, similarly, for all other test conditions. Because of the high degree of scatter, burn time results are not mentioned further in this article.

Water Vapor and Fluorine Effects

The main focus of this research was to determine if fluorine-containing compounds (SF_6, HF) affected the combustion history of boron particles. A set of experiments was also conducted with water vapor to confirm the results of previous work. Two different concentrations of each fluorine compound were investigated.

All of the experiments were conducted at a pressure of 8.5 or 34 atm in an oxidizing atmosphere of oxygen plus H_2O or fluorine additive. The ignition delay time of the third peak is shown in Figs. 14–17, where each oxidizer additive is compared to 100% oxygen to highlight specific results.

Figure 14 compares the third peak ignition delay of boron in water vapor/oxygen and pure oxygen. The ignition delay agrees at all temperatures to within the scatter of the data. No ignition is observed below 2100 K with water vapor and below 1900 K with oxygen.

Figure 15 displays the effect of SF_6 at 8.5 atm on third peak ignition delay. It was found that the addition of SF_6 had no measurable effect on the delay for peak 1 at 8.5 or 34 atm, indicating that the oxide layer removal rate was not increased. It was found, however, that the second peak was seldom seen in SF_6 experiments, which would suggest a change in the chemical pathway for the oxide removal reactions.

The addition of SF_6 at 8.5 atm (Fig. 15) has little effect on third peak ignition delay or on the ignition temperature limit. The limit for SF_6 is 1900 K, compared to 1900 K for the oxygen limit and 2200 K for the water vapor limit. When comparing data for 1, 2, and 3% mole fractions of SF_6 (not shown here) there is little discernible difference.

Figure 16 shows data for 1% SF_6 at 34 atm. There is a marked reduction in both ignition delay and ignition temperature limit for the SF_6 data compared to the 100% O_2 data. The ignition delay time is 200 μs lower at 1900 K and is about 100 μs lower at 2620 K. The ignition temperature limit for the SF_6 data is around 1400 K compared to 1900 K for pure oxygen data.

A side note on the SF_6 experiments concerns the profile of the photodiode signal. At temperatures close to the ignition temperature limit for SF_6, the third peak was sharply defined,

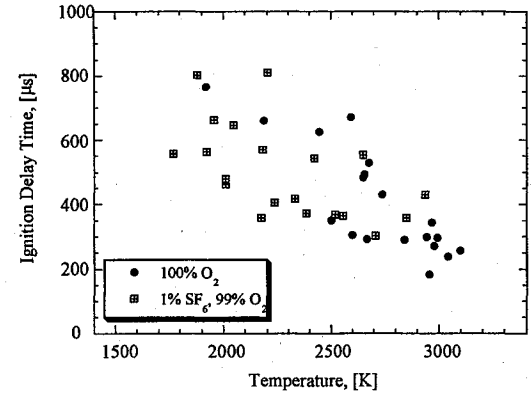

Fig. 15 Ignition delay time vs temperature of the third peak comparing SF_6 and O_2 for 20-μm boron particles at 8.5 atm.

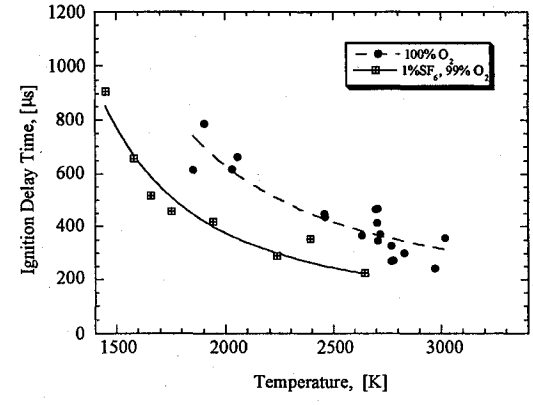

Fig. 16 Ignition delay time vs temperature of the third peak comparing SF_6 and O_2 for 20-μm boron particles at 34 atm.

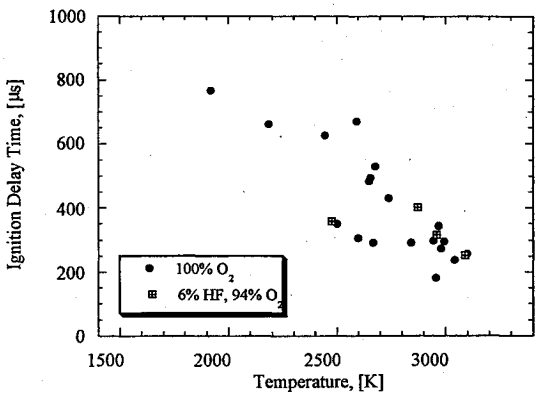

Fig. 17 Ignition delay time vs temperature comparing 6% HF and O_2 for 20-μm boron particles at 8.5 atm.

as compared to signals for pure O_2 at temperatures close to its ignition temperature limit.

Figure 17 illustrates the ignition delay results from the hydrogen fluoride experiments. The ignition delay times are very similar to the oxygen case, but with no ignition observed below 2450 K. There does not appear to be a significant decrease in ignition delay for HF with increasing temperature over the range studied. No difference in ignition delay was observed in tests conducted with 12% HF (data not shown).

Summary and Conclusions

It was previously found elsewhere[16] that boron undergoes two-stage ignition. In the first stage particle combustion begins, but is retarded by the presence of a liquid oxide layer.[2] The first stage ends when there is a runaway of oxide evaporation, which removes energy and extinguishes the particle. In the second stage the particle reignites and burns to completion.

We also have observed two-phase combustion, but have found that the first phase emission signal contains two peaks. From experiments conducted with 1-μm crystalline boron and <200-μm B_2O_3 particles, we conclude that parasitic particles on the surface of the 20-μm particles are not responsible for the two peak phenomenon. We instead suggest that removal of the boron oxide layer is responsible for both peaks.

Data from experiments in which SF_6 was added show little decrease in ignition delay time at 8.5 atm, but a significant effect at 34 atm. There is also a decrease in the ignition temperature limit at 34 atm from 1900 to 1400 K compared to pure oxygen data. The addition of HF or H_2O in experiments did not produce any significant effect.

Based on the experimental measurements of boron ignition in pure oxygen, the following conclusions can be drawn:

1) Amorphous boron has an ignition limit of 1425 K at pressures above 8.5 atm, and ignition delay times decrease with increasing temperature from 40 μs to an asymptotic value of 15 μs at 2000 K. Higher pressures have negligible effects.

2) For 20-μm crystalline particles, peaks 1 and 2 have a temperature ignition limit of 1900 K at pressures above 8.5 atm. The first and second peak ignition delay decreases with increasing temperature. Higher pressures do not affect the delay of either peak.

3) Twenty-μm crystalline particles (peak 3) ignite in less than 1 ms at temperatures above 2500 K and approach an ignition delay time limit of 250 μs at 3000 K for pressures above 8.5 atm. Increases in pressure show no measurable effects.

With additives, the results indicate the following:

1) Water vapor has no measurable effect on the ignition delay of 20-μm crystalline boron at 8.5 atm. There is, however, a slight increase in the ignition temperature limit.

2) Sulfur hexafluoride reduces the ignition delay time of amorphous boron.[1] SF_6 (1% in O_2) has little effect on the ignition delay time or the ignition temperature limit of 20-μm particles at 8.5 atm, but at 34 atm, there is a reduction in ignition delay and a reduction in the ignition temperature limit to 1450 K. Using different percentages of SF_6 does not affect the ignition delay. Therefore, it appears that fluorine atoms have a substantial effect on boron ignition at high pressures.

3) Hydrogen fluoride does not produce significant differences in ignition delay or burning time when compared to pure oxygen. Increasing the amount of HF does not change the results. Therefore, hydrogen fluoride does not observably enhance the chemical kinetics with boron or boron oxide, as predicted by other researchers.[19]

In future experiments, it is desirable to search for reasons why hydrogen fluoride does not change the ignition delay times. One possible theory is that it is necessary to dissociate HF, which cannot be done at the relatively low temperatures in the shock tube. Future experiments to create HF in situ using water vapor and sulfur hexafluoride together might answer this question.

Further chemical kinetic modeling for combustion of boron in F/O_2 atmospheres is required. It appears that fluorine not only assists in the combustion process, it appears to alleviate the long ignition delay at relatively low temperatures that has hindered the use of boron as a fuel.

Acknowledgments

This work was supported by the Office of Naval Research, under Contract N00014-93-1-0654 and an AASERT Graduate Student Support Contract N00014-93-1-1206. Dr. J. Goldwasser of the ONR is the Program Manager. We gratefully acknowledge the assistance of R. O. Foelsche, Ph.D. candidate, with experiments and interpretation of results, and the welcome assistance of C. Meyer and U. Yuki.

References

[1]Pirman, S. R., "Shock Tube Ignition and Combustion of Boron Particles in Oxygen with Fluorine Compounds," M.S. Thesis, Dept. of Mechanical and Industrial Engineering, Univ. of Illinois at Urbana–Champaign, Urbana, IL, 1994.

[2]King, M. K., "A Review of Studies of Boron Ignition and Combustion Phenomena at Atlantic Research Corporation over the Past Decade," *Combustion of Boron-Based Solid Propellants and Solid Fuels*, edited by K. K. Kuo and R. Pein, CRC Press, Boca Raton, FL, 1993, pp. 1–80.

[3]Besser, H. L., and Strecker, R., "Overview of Boron Ducted Rocket Development During the Last Two Decades," *Combustion of Boron-Based Solid Propellants and Solid Fuels*, edited by K. K. Kuo and R. Pein, CRC Press, Boca Raton, FL, 1993, pp. 133–178.

[4]Yetter, R. A., Rabitz, H., Dryer, F. L., Brown, R. C., and Kolb, C. E., "Kinetics of High-Temperature B/O/H/C Chemistry," *Combustion and Flame*, Vol. 83, No. 182, 1991, pp. 43–62.

[5]Roberts, T. A., Burton, R. L., and Krier, H., "Ignition and Combustion of Aluminum/Magnesium Alloy Particles in O_2 at High Pressures," *Combustion and Flame*, Vol. 92, Nos. 1,2, 1993, pp. 125–143.

[6]Roberts, T. A., "Shock Tube Ignition and Combustion of Aluminum/Magnesium Alloy Particles in Oxygen at High Pressure," Ph.D. Dissertation, Univ. of Illinois at Urbana–Champaign, Urbana, IL, 1993.

[7]*CRC Handbook of Chemistry and Physics*, 72nd ed., The Chemical Rubber Co., Cleveland, OH, 1991,1992.

[8]Incropera, F. P., and DeWitt, D. P., *Fundamentals of Heat and Mass Transfer*, 3rd ed., Wiley, New York, 1990.

[9]Chase, M. W., *JANAF Thermochemical Data*, 3rd ed., American Chemical Society, Washington, DC, 1985.

[10]*Journal of Physical and Chemical Reference Data*, Vol. 21, American Chemical Society, New York, 1992.

[11]Mohan, G., and Williams, F. A., "Ignition and Combustion of Boron in O_2/Inert Atmospheres," *AIAA Journal*, Vol. 10, No. 6, 1972, pp. 776–783.

[12]TAPP, Thermochemical and Physical Properties, Software Package, Version 1.0, E.S. Microware, Hamilton, OH, 1992.

[13]Nemodruk, A. A., and Karalova, Z. K., *Analytical Chemistry of Boron*, Ann Arbor–Humphrey Science Publishers, London, 1969,

pp. 5–16.

[14]Yeh, C. L., and Kuo, K. K., "Theoretical Model Development and Verification of Diffusion/Reaction Mechanisms of Boron Particle Combustion," *8th International Symposium on Transport Phenomena (ISTP-8) in Combustion*, Taylor and Francis, Washington, DC, 1995.

[15]Glassman, I., Williams, F. A., and Antaki, P., "A Physical and Chemical Interpretation of Boron Particle Combustion," *20th Symposium (International) on Combustion*, The Combustion Inst., Pittsburgh, PA, 1984, pp. 2057–2064.

[16]Macek, A., and Semple, J. M., "Combustion of Boron Particles at Atmospheric Pressure," *Combustion Science and Technology*, Vol. 1, 1969, pp. 181–191.

[17]Li, S. C., and Williams, F. A., "Ignition and Combustion of Boron in Wet and Dry Atmospheres," *23rd Symposium (International) on Combustion*, The Combustion Inst., Pittsburgh, PA, 1990, pp. 1147–1154.

[18]Macek, A., "Combustion of Boron Particles: Experiment and Theory," *14th Symposium (International) on Combustion*, The Combustion Inst., Pittsburgh, PA, 1972, pp. 1401–1411.

[19]Brown, R. C., Kolb, C. E., Yetter, R. A., Dryer, F. L., and Rabitz, H., "Kinetic Modeling and Sensitivity Analysis for B/H/O/C/F Combination Systems," *Combustion and Flame*, Vol. 101, No. 3, 1995, pp. 221–238.

[20]Megli, T. W., Krier, H., and Burton, R. L., "Shock Tube Ignition of Al/Mg Alloys in Water Vapor and Argon," *Experimental Heat Transfer, Fluid Mechanics, and Thermodynamics*, edited by M. D. Kelleher, R. K. Shah, K. R. Sreenivasan, and Y. Joshi, Vol. 2, Elsevier, New York, 1993, pp. 1097–1105.

[21]Anderson, J. D., Jr., *Modern Compressible Flow with Historical Perspective*, 2nd ed., McGraw–Hill, New York, 1990.

[22]Gordon, S., and McBride, B. J., "Computer Program for Calculation of Complex Chemical Equilibrium Compositions, Rocket Performance, Incident and Reflected Shocks, and Chapman-Jouguet Detonations," NASA SP-273, March 1976.

[23]Macek, A., and Semple, J. M., "Combustion of Boron Particles at Elevated Pressures," *13th Symposium (International) on Combustion*, The Combustion Inst., 1971, pp. 859–868.